



# IJRASET

International Journal For Research in  
Applied Science and Engineering Technology



---

# INTERNATIONAL JOURNAL FOR RESEARCH

IN APPLIED SCIENCE & ENGINEERING TECHNOLOGY

---

**Volume:** 11    **Issue:** I    **Month of publication:** January 2023

**DOI:** <https://doi.org/10.22214/ijraset.2023.48637>

[www.ijraset.com](http://www.ijraset.com)

Call:  08813907089

E-mail ID: [ijraset@gmail.com](mailto:ijraset@gmail.com)

# Chest X-ray Analysis using Deep Learning

Prof. Nisha P. Tembhare<sup>1</sup>, Prof. Puneshkumar U. Tembhare<sup>2</sup>, Prof. Chandrapal U. Chauhan<sup>3</sup>

<sup>1</sup>Assistant Professor, Department of Computer Technology, Yeshwantrao Chavan College of Engineering, Nagpur, Maharashtra, India

<sup>2</sup>Assistant Professor, Department of Computer Technology, Priyadarshini College of Engineering, Nagpur, Maharashtra, India

<sup>3</sup>Assistant Professor, Department of Computer Science and Engineering, Government College of Engineering, Chandrapur, Maharashtra, India

**Abstract:** Automatic recognition of key chest X-ray results to help radiologists with clinical workflow tasks like time-sensitive triage, pneumothorax (CXR) case screening and unanticipated discoveries. Deep learning models have become a promising prediction technique with near human accuracy, but usually suffer from a lack of explain ability. Medical professionals can treat and diagnose illnesses more precisely using automated picture segmentation and feature analysis. In this paper, we propose a model for automatic diagnosis of 14 different diseases based on chest radiographs using machine learning algorithms. Chest X-rays offer a non-invasive (perhaps bedside) method for tracking the course of illness. A severity score prediction model for COVID-19 pneumonia on chest radiography is presented in this study.

**Keywords:** Chest X-ray Analysis, Deep Learning

## I. INTRODUCTION

In many therapeutic applications, automated identification of significant abnormalities such as pneumothorax (PTX), pneumonia (PNA), or pulmonary edema (PE) on inch radiography (CXR) is an extensively explored area[1]. The Convolutional Neural Network is one of the most often used deep neural networks for image categorization (CNN). By using joint localization and classification algorithms to explicitly implement localization without the use of local annotation to direct image-level classification, we both address the current drawbacks, including the lack of interpretability and the requirement for costly local annotation, in this work. The respiratory system's key organ, the lung serves as an organ for exchanging oxygen from the air and carbon dioxide from the blood. As a result, they are crucial parts of the respiratory system in humans. The respiratory system is immediately impacted by lung injury, which has the potential to be fatal. Pleural effusion alone accounts for 2.7% of other respiratory disorders in Indonesia, with an estimated global frequency of more than 3,000 cases per million people annually.

As the first nation examines stay-at-home strategies [1], deaths from COVID-19 continue to rise [2]. The growing pressure of the pandemic on health systems around the world Many doctors have turned to new strategies and techniques. Chest x-ray (CXR) provides a non-invasive (potentially bedside) tool for monitoring disease progression [3]. In early March 2020, Chinese hospitals used artificial intelligence (AI)-assisted computed tomography (CT) image analysis to screen for COVID-19 cases and simplify diagnosis [4]. Since then, many teams have launched AI initiatives to help triage COVID-19 patients (i.e., discharge, general admission, or ICU care) and allocate hospital resources (i.e., from direct non-invasive ventilation to invasive ventilation). [5,6]. Although these latter tools use clinical data, there is still a lack of practically deployable CXR-based prediction models.

## II. RELATED WORK

This section gives a quick explanation of the algorithms utilised in this work, CNN and its Component, as well as a review of various other studies that employed comparable algorithms to complete a goal, such as classifying chest radiographs.

### A. Classifying Chest X-ray Images on CNN

In the medical area, particularly in the identification of anomalies based on X-ray pictures, machine learning techniques, particularly deep learning, have gained popularity recently. One of the experiments examined the accuracy of the rice field in 10 situations for the diagnosis of 14 illnesses based on chest radiography and CNN, as carried out by [6]. (Including edema, pleural effusion, pneumonia, etc.) Radiation exposure (after special test). Similar work was done by [7] and [8] and these were also obtained. Reliable accuracy for 14 diseases.

### B. Convolutional Neural Network

Artificial neural networks (ANNs), sometimes referred to as neural networks or CNNs, are one form of ANN (NN). It is a machine learning method that draws inspiration from the organisation of the human brain (also known as deep learning because it often includes numerous layers). network of neurons. CNNs and standard NNs are quite similar. In contrast to a standard NN, a CNN has a specific initial layer called the convolution layer that harvests data, particularly picture characteristics. As a result, tasks including image classification, object identification, and picture segmentation are frequently carried out using CNNs. Using Computer Vision, the unstructured data seen in photos and other unstructured data is where this algorithm excels [9]. CNNs are generally divided into convolution layers, combination layers and fully connected layers [10]

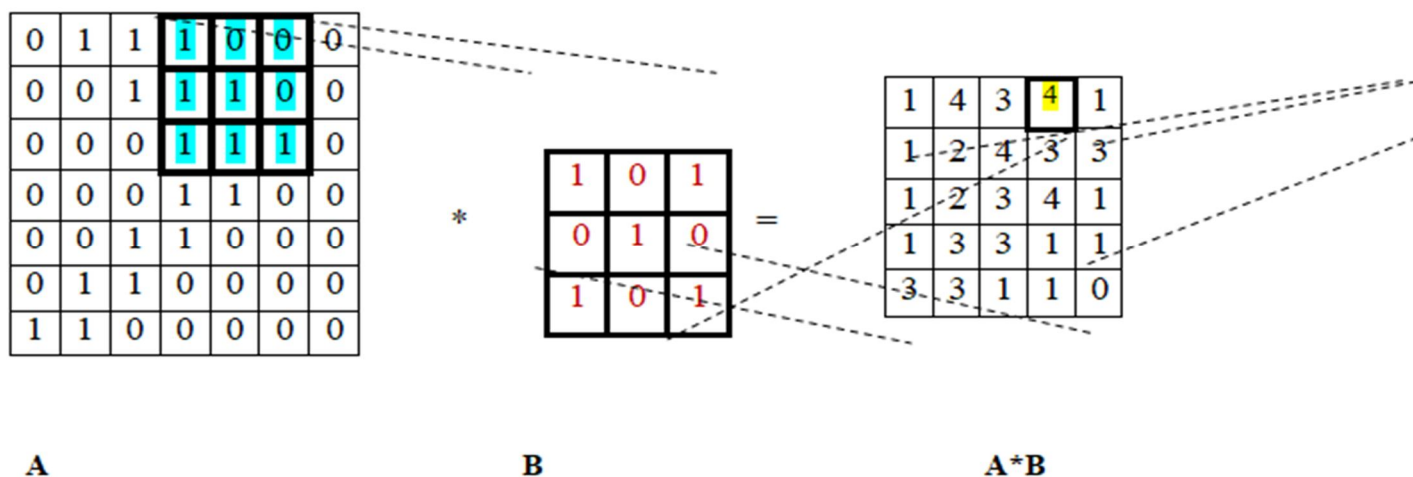


Figure 1: An example of how convolution works

The feature maps can be nonlinearly transformed by applying a nonlinear activation function to this layer [12]. The ReLU is a typical nonlinear activation function (Revised Linear Unit), Shown in equation (1)

$$(x) = \max(0, x) \tag{1}$$

Where  $x$  is the output of the neuron (or value in the future map),  
if  $x \leq 0$ , then  $x = 0$  and if  $x > 0$ , then  $x = x$ .

### C. Pooling Layer

A CNN's fusion layer, also known as a subsampling layer, lowers the dimensionality of feature maps by choosing pixel values in accordance with predetermined criteria. Maximum pooling and average pooling are two frequently used pooling layer methods [13]. By maintaining the greatest value in the feature map, maximum merging operates (as shown in Figure 2). In contrast, the average merge searches for the feature map's average value (it is called a global merge if it returns only one value per feature map, or it can also use a kernel configured to return multiple values).

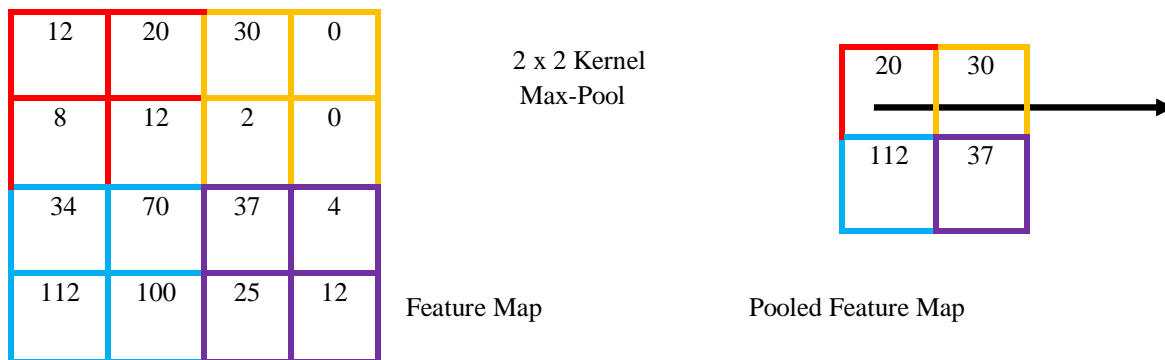


Figure 2. An example of the pooling procedure (max-pool)

### III. METHODOLOGY

There are many steps in this section. We first provide a brief description of the pre-processing methods employed on the data in this work before moving on to the CNN architecture and suggested meta-parameters. Finally, we discuss model implementation strategies, model interpretation methods, and performance measures at the end of this section.

#### A. Dataset

The biggest chest radiography dataset, Chest X-ray, has a total of 112,120 pictures from 30,805 patients with a variety of advanced lung illnesses. It was used in this study. taken from Kaggle: Chest CT Scan Images [7]. Based on the kind of sickness and the level of health, this dataset is classified into 14 groups. Images were resized to 1024 by 1024 pixels, saved in PNG format, then labelled with one or more tags (overlapping with other diagnoses). They were acquired by means of natural language processing methods from radiologist reports. 81,176 data samples from X-ray scans were used in the investigation. With 1250 photos per dataset and 14 distinct classes, it provides X-ray images of 14 different lung diseases.

#### B. Proposed CNN Architecture

The visual geometry group's VGG19 CNN model was utilised in this study [17]. A deep CNN model with 19 layers is called VGG19 (16 convolutional layers and 3 FC layers).

The ImageNet dataset served as the basis for the initial parameters of the VGG19 model, which was employed in this work (also called pre-trained model). a convolution layer modified to fit the applied data set in the model architecture's top layer (fully linked layer).

#### C. Performance Metrics for Evaluation

The model's performance on the test set is evaluated using the confusion matrix utilising several criteria, including accuracy, sensitivity, and specificity

|              |          |                 |                |
|--------------|----------|-----------------|----------------|
|              |          | Predicted Label |                |
|              |          | Negative        | Positive       |
| Actual Label | Negative | True Negative   | False Positive |
|              | Positive | False Negative  | True Positive  |

Figure 4. Image of the confusion matrix.

- **Accuracy:** It shows the accuracy of the model. It is the ratio of total actual predictions to total predictions.

$$Accuracy = \frac{TP+TN}{(TP+TN+FP+FN)} \tag{2}$$

- **Sensitivity:** Measurement using sensitivity (or true positive rate) The ability of the model to correctly classify positive samples.

$$Sensitivity = \frac{TP}{FN + TP} \tag{3}$$

- **Specificity:** The model's ability to accurately categorise negative samples is measured by its specificity (also known as true negative rate).

$$Specificity = \frac{TN}{TN + FP} \tag{4}$$

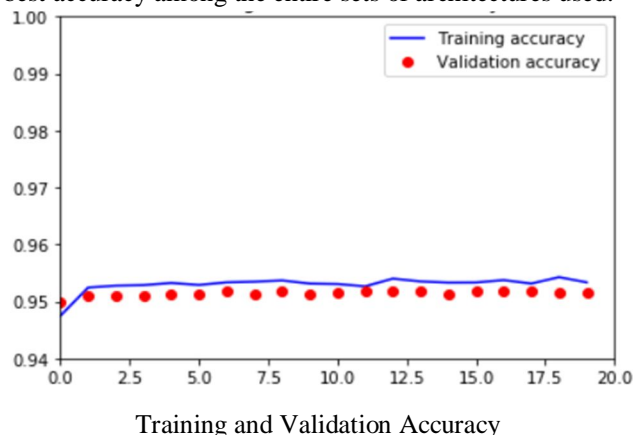
D. Proposed & Comparative Architectures

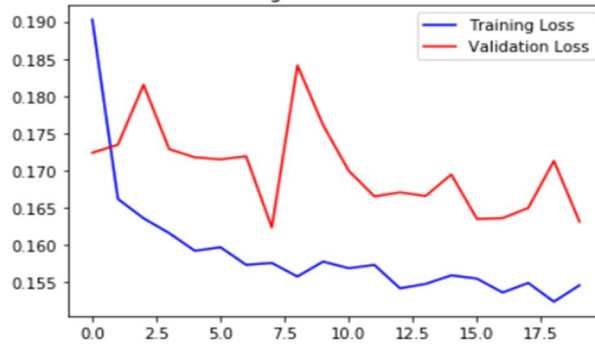
- 1) *Image Network*: We tested various architectures to pre-process image networks with pre-trained weights from ImageNet. The architectures evaluated are as mentioned below:
  - a) *VGG 19*: VGG 19 comprises two parts, VGG stands for Visual Geometry Group while 19 represents the deep architecture formed by 19 layers of convolutional neural networks. This is a pre-trained architecture that can classify 1000 different objects. VGG 19 accepts RGB input in the 224 by 224 resolution. The pre-processing that the input image in VGG 19 goes through is subtracting the mean RGB value from every pixel. The VGG deep layer network consists of 16 layers of CNNs along with three complete layer connections ending with a softmax layer.[18] The width of the convolution layer in the starting is 64 channels which increase by a factor of 2 till it reaches 512 channels. The initial two fully connected layers are made up of 4096 channels while the last one performs the ImageNet Large Scale Visual Recognition Challenge (ILSVRC) classification, so this has a thousand channels.[18] The architecture also uses ReLU to bring in non-linearity and decrease the computational time and improve the accuracy.
  - b) *Inception V3*: Inception V3 is constructed by making some changes in the Inception V2 architecture. The first change is that the starting two 7\*7 convolution layer is factored into multiple 3\*3 convolution layers. This model is made up of multiple convolutional layers, average and max pooling, dropout, and concat along with fully connected layers. It also uses batch normalization in the model and also to activates the inputs.[19] On the ImageNet dataset, this architecture gained an accuracy above 78.1%. This was developed by Google. Inception V3 has 42 layers but still, its computational time is very less.[19]
  - c) *ResNet 50v2*: ResNet development was inspired by the VGG networks. This is developed by changing the 34-layer net to the 3-layer bottleneck which forms the 50-layer ResNet structure. This is a deep structure consisting of 50 layers. Similar to VGG it can classify 1000 different objects and also accepts an input size of 224\*224.[20] ResNet is less complicated than VGG as it has fewer filters. In this structure, the down sampling is done by a convolutional layer having 2 strides. It also has an average pooling layer and a softmax layer.[20]
  - d) *Inception-ResNet*: It is a deep neural network architecture that is 164 layers deep and can classify 1000 different objects. This accepts an image as input in the resolution 299\*299. This is different from traditional Inception as batch normalization is applied only on the top layer and not on the summation layers.[21] The filters used should be not above 1000 because it is noticed that it starts to show irregularities. It contains a convolution network, average pooling, softmax, dropout, stem, and reduction.[21]

E. Model Comparison

We ran various tests on the training set, training the suggested technique and benchmark models, and afterward validating the model with the validation set.

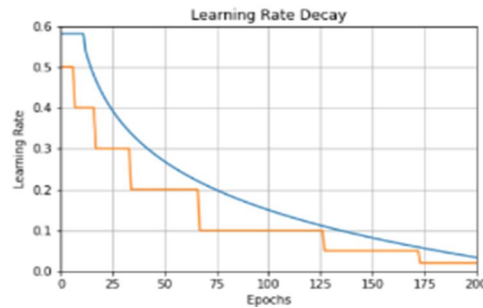
- 1) *Validation Loss*: While evaluating we observed that different architectures behave differently on being trained over multiple epochs. VGG 19 validation loss was minimum which reduced from 3 to 0.8. While the other two algorithm validation losses did not improve much and remained almost constant over entire training. ResNet 50 although improved drastically from 6.3 to 2, but could not improve further.
- 2) *Validation Accuracy*: The accuracy parameter portrays the model's efficiency and performance. It is evident from the below graph that VGG19 achieved the best accuracy among the entire sets of architectures used.





Training and Validation Loss

3) *Training Methodology:* We have trained our networks with Adam optimizer. Adam is a momentum-based gradient descent approach that uses adaptive first-order and second-order moment estimation. All our models were developed and trained using TensorFlow version 2.6. In our experiments, we used the beta\_1=0.874, beta\_2=0.935, epsilon=1e-6.5, and the learning rate decayed over every 3 epochs with an exponential rate of 0.56

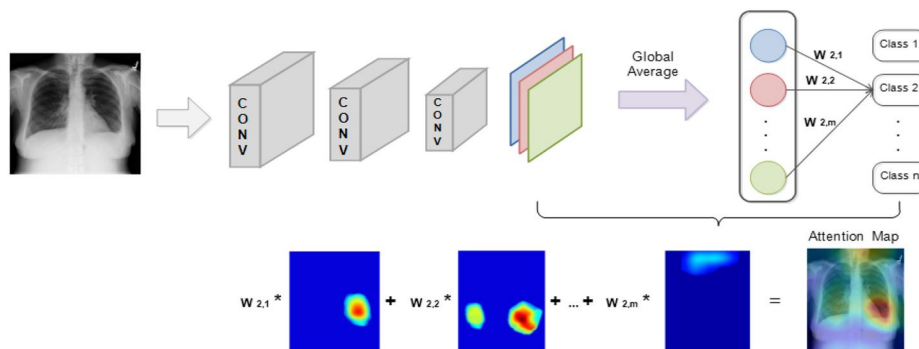


Learning rate decay used in our study

| Model             | Recall | F1-Score | ROC Curve AUC | Recall AUC |
|-------------------|--------|----------|---------------|------------|
| Inception v3      | 0.874  | 0.892    | 0.883         | 0.942      |
| Inception- ResNet | 0.832  | 0.990    | 0.904         | 0.955      |
| VGG19             | 0.838  | 0.992    | 0.908         | 0.954      |
| ResNet50 v2       | 0.848  | 0.958    | 0.898         | 0.950      |

Confusion Matrices (CMs) and performance measures of different models.

#### IV. EXPERIMENT RESULT



Disease localization using class activation mapping.

We combined all four models on a virtual machine deployed on the Microsoft Azure platform to see how effective they are. For simulations, the Python programming language is utilized. In DenseNet, Inception, VGG-19, and ResNetV2

| Model            | Accuracy | Loss (Cross-Entropy) |
|------------------|----------|----------------------|
| VGG19            | 94.2     | 0.62                 |
| ResNet 50 v2     | 75.5     | 2.0                  |
| Inception v3     | 68.4     | 3.0                  |
| Inception-ResNet | 79.4     | 1.8                  |

Model Accuracy and Loss of all models

| Model             | Total Epoch | Validation Loss | Training Time (Epoch) | Time (Best Model) |
|-------------------|-------------|-----------------|-----------------------|-------------------|
| VGG19             | 200         | 0.62            | 44s                   | 4268s             |
| ResNet 50 v2      | 200         | 2.0             | 43s                   | 3999s             |
| Inception- ResNet | 200         | 1.8             | 51s                   | 499s              |
| Inception v3      | 200         | 3.0             | 45s                   | 4519s             |

Best model Verification by Time

The study results show that VGG19 and DeBERTa-v2 models inherently performed better on the classification task. So, we came out to the conclusion to choose this model for further fine-tuning. This is achieved by varying different hyper parameters. Making these improvements it is seen that our VGG19 performance also increased up as evident.

### V. CONCLUSION

In summary, to correctly identify the diagnosis of multiple diseases and identify particular symptoms of disease, integrated modifications in the CNN deep model structure and fine-tuning of the model using the Optimization technique throughout the model training process are required. To evaluate the suggested approach, we used a number of deep CNN models (VGG16, VGG19, Inception V3, ResNet34, ResNet50, ResNet101) with various module layouts and layer counts. Our results suggest that the overall performance of deep CNN models keeps improving with the superimposition of improvement stages. Structure modifications produce the most increase in prediction accuracy for single CNN models among the three phases.

The proposed ensemble model can deliver good results even for the objective of disease localization by precisely presenting an attention map that highlights lung region regions that are suspected of having disease. Results from qualitative and quantitative research demonstrate that our technique outperforms other reducing algorithms in terms of performance.

### REFERENCES

- [1] S. A. Nasution, "Skrining Makroskopis Cairan Pleura dari Efusi Pleura di Unit Laboratorium Patologi Anatomi Rumah Sakit Umum Pendidikan Haji Adam Malik Medan," J. AnLabMed Vo.1 No.1 Desember, 2019.
- [2] I. Puspita, T. Umiana Soleha, and G. Berta, "Penyebab Efusi Pleura di Kota Metro pada tahun 2015," J AgromedUnila , vol. 4, p. 25, 2017.
- [3] J. T Puchalski, "Mortality of Hospitalized Patients with Pleural Effusions," J. Pulm. Respir. Med., vol. 04, no. 03, 2014, doi: 10.4172/2161-105x.1000184.
- [4] P. Rajpurkar et al., "CheXNet: Radiologist Level Pneumonia Detection on Chest X-Rays with Deep Learning," Nov. 2017.
- [5] P. Rajpurkar et al., "Deep learning for chest radiograph diagnosis: A retrospective comparison of the CheXNeXt algorithm to practicing radiologists," PLoS Med., vol. 15, no. 11, Nov. 2018, doi: 10.1371/journal.pmed.1002686.
- [6] X. Wang, Y. Peng, L. Lu, Z. Lu, M. Bagheri, and R. M. Summers, "ChestX-ray8: Hospital scale chest X-ray database and benchmarks on weakly-supervised classification and localization of common thorax diseases," in Proceedings - 30th IEEE Conference on Computer Vision and Pattern Recognition, CVPR 2017, May 2017, vol. 2017-Janua, pp. 3462-3471, doi: 10.1109/CVPR.2017.369.
- [7] H. Wang and Y. Xia, "ChestNet: A Deep Neural Network for Classification of Thoracic Diseases on Chest Radiography," 2018.
- [8] Ž. Knok, K. Pap, and M. Hrnčić, "Implementation of intelligent model for pneumonia detection," Teh. Glas., vol. 13, no. 4, pp. 315-322, 2019, doi: 10.31803/tg- 20191023102807.



- [9] I. B. L. M. Suta, R. S. Hartati, and Y. Divayana, "Diagnosa Tumor Otak Berdasarkan Citra MRI (Magnetic Resonance Imaging)," *Maj. Ilm. Teknol. Elektro*, vol. 18, no. 2, Jun. 2019, doi: 10.24843/mite.2019.v18i02.p01.
- [10] L. Devnath, S. Luo, P. Summons, and D. Wang, "Tuberculosis (TB) Classification in Chest Radiographs using Deep Convolutional Neural Networks," *Int. J. Adv. Sci. Eng. Technol.*, vol. ISSN, no. 3, pp. 2321–9009, 2018.
- [11] R. H. Abiyev and M. K. S. Ma'aitah, "Deep Convolutional Neural Networks for Chest Diseases Detection," *J. Healthc. Eng.*, vol. 2018, 2018, doi: 10.1155/2018/4168538.
- [12] L. A. Andika, H. Pratiwi, and S. S. Handajani, "Klasifikasi Penyakit Pneumonia Menggunakan Metode Convolutional Neural Network Dengan Optimasi Adaptive Momentum," *Indones. J. Stat. Its Appl.*, vol. 3, no. 3, pp. 331–340, 2019.
- [13] O. Stephen, M. Sain, U. J. Maduh, and D. U. Jeong, "An Efficient Deep Learning Approach to Pneumonia Classification in Healthcare," *J. Healthc. Eng.*, vol. 2019, 2019, doi: 10.1155/2019/4180949.
- [14] R. Rokhana et al., "Convolutional Neural Network untuk Pendeteksian Patah Tulang Femur pada Citra Ultrasonik B-Mode," *JNTETI*, vol. 8, no. 1, 2019.





10.22214/IJRASET



45.98



IMPACT FACTOR:  
7.129



IMPACT FACTOR:  
7.429



# INTERNATIONAL JOURNAL FOR RESEARCH

IN APPLIED SCIENCE & ENGINEERING TECHNOLOGY

Call : 08813907089  (24\*7 Support on Whatsapp)